

# New chemical treatment for bioactive titanium alloy with high corrosion resistance

S. SPRIANO\*, M. BRONZONI, F. ROSALBINO, E. VERNÈ

SMIC Department, Polytechnic of Turin, Corso Duca degli Abruzzi, 24 - 10129 Turin, Italy  
E-mail: [silvia.spriano@polito.it](mailto:silvia.spriano@polito.it)

It was recently claimed that titanium metal and its alloys can bond to the living bone, without being coated by apatite (VPS coatings), but by being chemically and heat-treated. The bioactivity of treated titanium is of interest because of the opportunity to obtain orthopaedic or dental implants presenting, at the same time, high toughness, strength and fatigue resistance as well as bone-bonding ability. The bioactive behaviour of the treated implants is due to the presence of a modified surface, which, during soaking in body fluid, promotes the precipitation of apatite. The apatite formed is strongly bonded to the substrate and promotes living bone bonding. In this work were characterised samples of Ti-6Al-7Nb alloy with surfaces presenting a different chemical and mechanical state. The aim of the research was twofold. The first objective was to characterise chemically and heat-treated samples with different surface topography, in order to define the best conditions for osteogenic integration. The second aim was to assess the corrosion behaviour of the bioactive implants, because they expose a microporous and quite thin modified surface layer. No-treated and passivated samples, with a surface state closed to that nowadays used on implants, were used as reference. The surface structure, morphology, electrochemical behaviour and bioactivity of the different samples were assessed by means of XRD, SEM-EDS, anodic polarizations, open circuit measurements and *in-vitro* tests. Results evidence that it is possible to modify the surface of the Ti-6Al-7Nb alloy in order to obtain the formation of a bioactive layer and that the substrate roughness influences the characteristics of the surface layer formed. It was also evidenced that the as treated surfaces present inadequate corrosion behaviour, so a new two-step chemical treatment has been developed in order to obtain a bioactive material with good corrosion resistance.

© 2005 Springer Science + Business Media, Inc.

## 1. Introduction

The bioactivity of thermochemical treated titanium and titanium alloys engaged the attention of some research groups during the last years [1–4], because of the interest related to a material presenting, at the same time, high toughness, strength and fatigue resistance as well as bone-bond ability [5–6].

Different chemical treatments were proposed in literature, by using H<sub>2</sub>O<sub>2</sub> [7], HCl and H<sub>2</sub>SO<sub>4</sub> [8] as etching solutions, but most of the experiments were performed by etching in concentrate NaOH solution and subsequent thermal treatments at 500–800 °C [9]. The authors underlined the formation, on the treated samples, of a sodium titanate layer, which showed a bioactive behaviour during soaking *in vitro* in simulated body fluid (SBF), by the precipitation of an apatite layer. The apatite formed on the treated titanium is much more strongly bonded to the substrates than that precipitated

on traditional bioactive materials (Bioglass 45S5-type, glass-ceramic apatite-wollastonite and sintered dense hydroxyapatite) [10]. This seems to be related to the graded interface structure of the apatite and of the titanate layer to the Ti metal substrates [11, 12]. The proposed mechanism, in order to explain the bioactivity of treated samples, involves the transformation of the alkali titanate layer into TiO<sub>2</sub> hydrogel, via release of alkali ions into SBF and ion exchange with H<sub>3</sub>O<sup>+</sup> ions from the solution [17]. Kokubo *et al.* [13, 14] registered good bone bonding ability of treated titanium implants by *in vivo* tests; their results evidenced also that both alkali and heat treatment are essential in order to induce bioactivity *in vivo*.

An analogous treatment, by using more diluted NaOH solutions, was used with success on pure tantalum [15]. Hydroxyapatite formation on treated tantalum was detected after soaking in SBF and bone-bonding

\*Author to whom all correspondence should be addressed.

ability at 16 weeks after implantation was observed [16]. On the other hand alkali treated 316L stainless steel and Co-Cr-Mo alloys did not evidence any bioactivity [17].

The mechanical state of titanium surface is another critical parameter in order to obtain stable implants. Cement and cementless fixation implants required quite different surface finishing state. Considering cementless fixation, it was shown that macro and microscopic roughness are determinant parameters in influencing type and orientation of cells attaching. The cause of this behaviour is still an open problem: it could be a pure geometrical factor or a function of alterations in surface chemistry encumbered during surface preparation [18]. In any case recent *in vivo* studies on the osteogenic response to smooth and blasted cementless implants [19] confirmed that the former result in fibrous interfaces and poor fixation, while medium size rough surfaces ( $R_a \approx 4 \mu\text{m}$ ) have a higher push-out strength (35 MPa). On the other hand considering cement fixed implants it was assessed that, in order to minimise cement abrasion and micromotions at the stem-cement interface, stems should have a polished surface [20].

An interesting aspect, not yet investigated in detail, is the effect of the presence of bioactive porous layers on surfaces with controlled state of roughness, in order to combine favourable surface topography and bioactive ability. So the aim of this work was twofold. The first objective was to characterise alkali treated samples with different surface topography: mirror polished and sandblasted surfaces were considered. Moreover, particular attention was also devoted to the corrosion resistance of the porous layer in order to evaluate if its protection ability was so good as that of the native oxide or of the passive one. A new two-step chemical treatment has been developed in order to obtain a bioactive material with good corrosion resistance. No-treated and passivated samples, with a surface state closed to that nowadays used on implants, were used as reference. The surface structure, morphology, electrochemical behaviour and bioactivity of the different samples were assessed. Ti-6Al-7Nb alloy was used for these experiments, according to its good performance and wide use as implant material.

## 2. Experimental

The Ti-6Al-7Nb alloy was produced by the Sulzer Orthopedics according to ISO 5832-11. The subsequent different surface treatments were considered. Two different mechanical finitures: mirror polishing (*M* series) and corindone sandblasting (*B* series). Mirror polishing was performed by grinding, using  $1 \mu\text{m}$  diamond paste as last finiture. Sandblasting was performed by using 60 grit particles at the pressure of 6 atm.

Chemical treatments were performed on both these sample series. Alkali treatment was performed by etching in 5 M NaOH at  $60^\circ\text{C}$  for 24 h, analogously to what reported in literature [17]. Mirror polished and alkali treated samples will be called *MA* series, while sandblasted and alkali treated samples will be called *BA*

TABLE I Legend of the different mechanical, chemical and thermal treatment employed

Mechanical treated samples		Mirror polished Blasted	M B
Mechanical and chemical treated samples	Single step	M + alkali treatment	MA
		B + alkali treatment	BA
		M + passivation	MP
	Two steps	B + passivation	BP
		MP + alkali treatment	MPA
		BP + alkali treatment	BPA
Mechanical, chemical and heat treated samples	Single step	MA + $600^\circ\text{C}$ 1 h	MA600
		MA + $700^\circ\text{C}$ 1 h	MA700
		MA + $800^\circ\text{C}$ 1 h	MA800
		BA + $600^\circ\text{C}$ 1 h	BA600
		BA + $700^\circ\text{C}$ 1 h	BA700
		BA + $800^\circ\text{C}$ 1 h	BA800
	Two steps	MPA + $600^\circ\text{C}$ 1 h	MPA600
		BPA + $600^\circ\text{C}$ 1 h	BPA600

series. Passivation treatment was performed by using 30%  $\text{HNO}_3$  for 30 min (*MP*, *BP* series). A new two-step chemical treatment has been tested: it includes passivation, as first step, and alkali treatment, as second step, performed as previously described (*MPA*, *BPA* series).

Some samples treated by alkali or two step etching were dried at  $40^\circ\text{C}$  in air for 24 h and heat treated in furnace at  $600\text{--}800^\circ\text{C}$  for 1 h. A number, corresponding to the heating temperature set in the furnace, will be reported in order to call the specimens in a short while (*MA600*, *BA600*, *MPA600*, *BPA600* and so on).

Table I summarises the above mentioned sample series.

Surface crystalline structure was investigated by X-ray diffraction analysis (X'Pert Philips diffractometer), using the parallel beam camera geometry (XRD-PB) and the  $\text{Cu-K}\alpha$  incident radiation. The incident angle was set at 1.5 degrees.

Surface morphology and composition were assessed by scanning electron microscopy (SEM Philips 525 M) and energy dispersion spectrometry (EDS Philips-EDAX 9100).

Electrochemical behaviour evaluation was performed in Ringer solution (NaCl 9 g/l,  $\text{CaCl}_2$  0.24 g/l, KCl 0.43 g/l,  $\text{NaHCO}_3$  0.2 g/l), maintained at  $(25 \pm 1)^\circ\text{C}$ , by means of cyclic polarisation and open-circuit potential experiments. In cyclic polarisation measurements, the potential sweep rate was 1 mV/s starting from the open circuit potential and moving in anodic direction up to +3.0 V, followed by a reverse sweep, which finished when the protection potential,  $E_{\text{prot}}$ , was reached. Open circuit potentials were recorded every 3 min for a period of 72 h. All potentials were measured against a saturated calomel electrode (SCE).

Soaking in standard SBF solution [17] was performed for 7 and 14 days in order to investigate the bioactivity of the different samples.

## 3. Results

### 3.1. Surface morphology and composition

The composition of the mechanical treated materials (*M*, *B*) was checked by EDS analysis and it was found

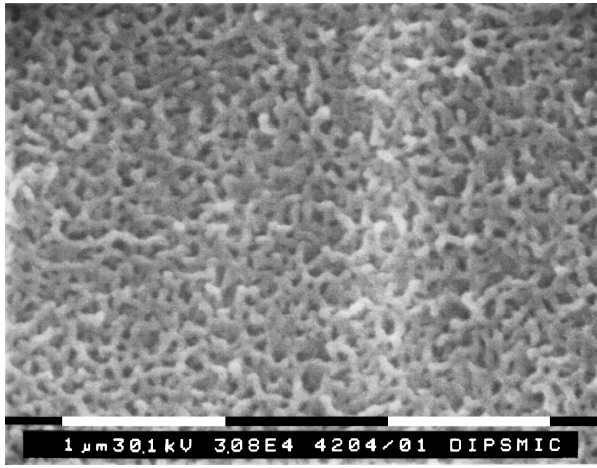


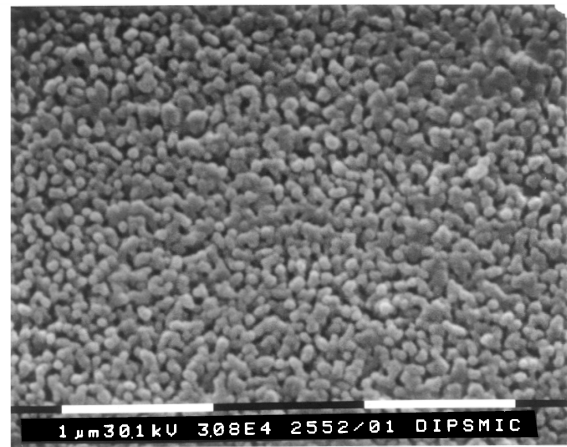
Figure 1 Surface morphology of BPA samples (SEM microphotograph).

quite close to the nominal one. Some alumina particles were randomly observed on the surface of sandblasted samples.

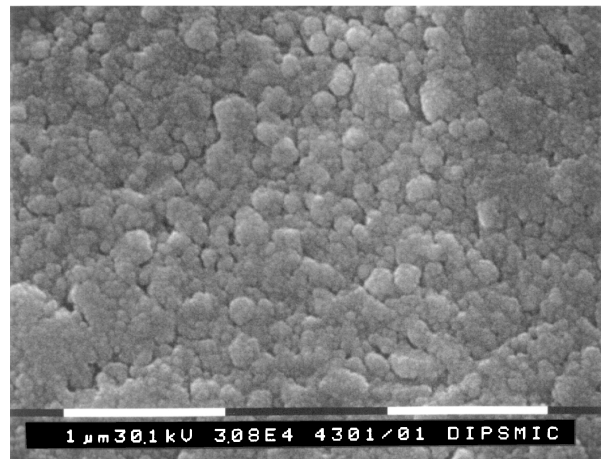
The effects of thermochemical treatments on the surface morphology were investigated by observing as first chemically treated samples. No evident modification in morphology or composition of the samples has been detected, by means of SEM-EDS analysis, after passivation in  $\text{HNO}_3$  (*MP*, *BP* series).

On the contrary the presence of a microporous layer was observed on the NaOH treated samples, analysed before heat treatment (*MA*, *BA* series). It was formed by small almost spherical particles with a medium diameter of  $0.1 \mu\text{m}$ , arranged on the surface by forming micropores. Also in the case of sandblasted, passivated and alkali treated samples the surface morphology is quite alike (Fig. 1-*BPA* series). Also mirror polished, passivated and alkali treated samples (*MPA* series) show a similar morphology, but it is on a smaller scale and it is hardly observable by SEM. The estimated size of spherical particles is about 30 nm. A hardly detectable Na signal resulted from EDS analysis on the alkali treated samples, but it was too weak in order to perform a detailed investigation by means of this technique.

Furthermore the morphology of heat treated samples was observed. In the case of alkali and heat treated polished specimens (*MA600* samples), the surface looks like covered by spherical particles, showing a quite regular shape and about 120 nm in diameter (Fig. 2(a)). Otherwise coarse aggregates appear after the heat treatment on passivated and alkali-treated samples (*MPA600* series) forming a quite dense layer (Fig. 2(b)). There is a wide distribution in aggregates size from 80 to 500 nm, and quite small particles (30 nm-diameter) are visible as sub-elements of the aggregates. Also in the case of sandblasted samples the heat treatment at  $600^\circ\text{C}$  caused a densification of the porous surface (Fig. 3(a)–(b) *BA600*, *BPA600* series), and the growth of a homogeneous layer consisting of almost spherical and thickened particles can be observed. They are about 80 nm in diameter. In case of a previous passivation treatment there is no evident modification of the surface morphology. No compositional changes were evidenced by means of EDS after any heat treatment.



(a)



(b)

Figure 2 Surface morphology of *MA600* (a) and of *MPA600* (b) samples.

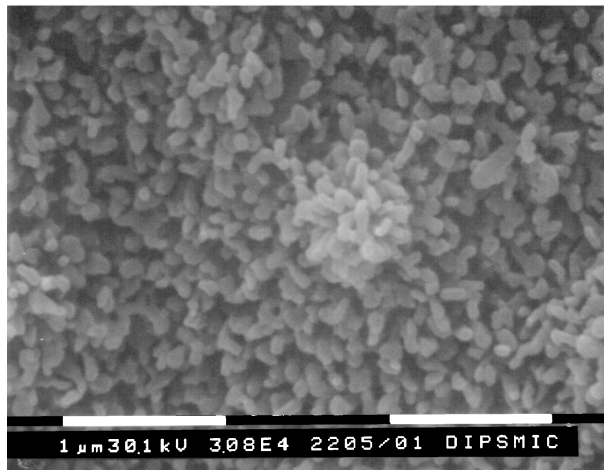
It can be concluded that the thermochemical process produced a submicrometric textured layer and that differences in morphology as a consequence of the various treatments, with or without passivation, are much more evident in the case of mirror polished respect to blasted surfaces.

Heat treatments at higher temperature ( $700\text{--}800^\circ\text{C}$ ) produce darker surfaces and the growth in dimension of the surface particles on all the sample series, producing a dense aspect of the surface. Considering that the aim of this research work is to test the performance of microtextured and microporous surfaces, these samples were not characterized in details.

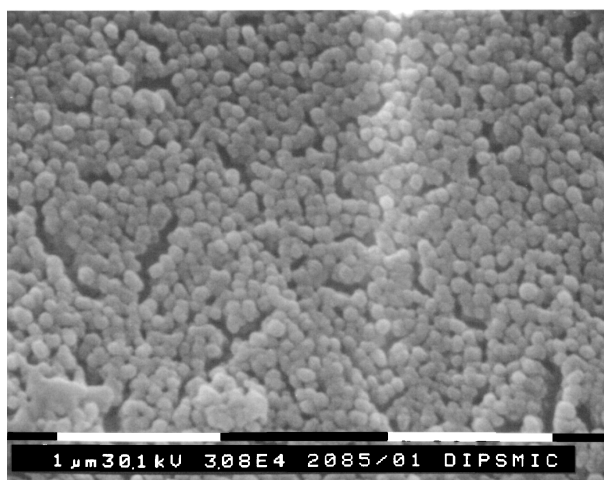
### 3.2. Surface structure

According to these morphological observations, the XRD-PB diffraction analysis evidenced some differences on smooth and blasted samples, as can be observed by comparing Figs. 4 and 5.

On *MA* samples no diffraction peak, apart from those related to titanium substrate, could be evidenced (Fig. 4—curve a). A broad signal centred at about 45 degrees is present on the diffraction pattern obtained on the *MA600* sample (Fig. 4—curve b) and heat treatment at higher temperature ( $700\text{--}800^\circ\text{C}$ ) are necessary in order to obtain crystalline surface phases (Fig. 4—curves c and d). The diffraction peaks observed on *MA700* and *MA800* samples can be attributed to rutile and



(a)



(b)

Figure 3 Surface morphology of BA600 (a) and BPA600 (b) samples.

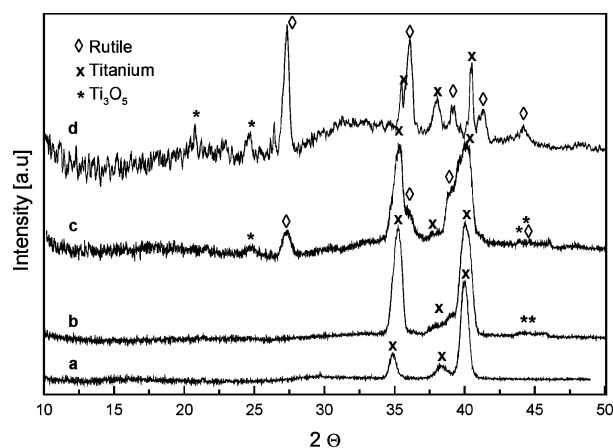


Figure 4 PB-XRD patterns related to MA (curve a), MA600 (curve b), MA700 (curve c), MA800 (curve d) samples.

to  $\text{Ti}_3\text{O}_5$  monoclinic phase. The signals of the  $\text{Ti}_3\text{O}_5$  phase could also be referred to a sodium containing oxide ( $\text{Na}_2\text{Ti}_3\text{O}_7$ ), but according to the low evidence of Na registered on our samples we preferred a different awarding. On the MA800 sample rutile peaks are so intense that they are more pronounced than the signals of the titanium substrate.

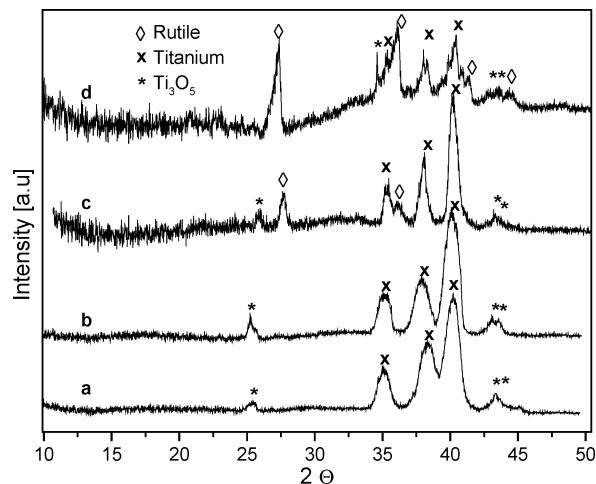


Figure 5 PB-XRD patterns related to BA (curve a), BA600 (curve b), BA700 (curve c) and BA800 (curve d) samples.

On the contrary on sandblasted samples the  $\text{Ti}_3\text{O}_5$  monoclinic phase can be observed also after NaOH etching and before heat treatment (BA) (Fig. 5—curve a). It grows in volume fraction after heat treatment at  $600^\circ\text{C}$  (BA600) (Fig. 5—curve b) and it is coupled with rutile on the samples treated at 700 and  $800^\circ\text{C}$  (BA700 and BA800) (Fig. 5—curve c and d). No diffraction signal was detected on BP samples, apart from those related to titanium substrate, while the samples treated by two-step chemical etching (BPA, BPA600) present the same structure than the analogous single step ones (BA, BA600).

The diffraction peaks related to the titanium substrate are, in the case of sandblasted samples, in a ratio of intensity closed to the theoretical random pattern. They do not significantly change in the diffraction patterns related to the different heat treated samples, a part from a reduction in half height width due to the growth in dimension of the crystals on BA800 sample. The difference in intensity of the titanium substrate peaks observable on mirror polished samples is to be referred mainly to a grained texture due to surface preparation. It is variable from specimen to specimen so it cannot be used in order to obtain structural information [21]. No influence of the crystallographic texture of the substrate on the treated surface structure will be relieved. Considering that the objective of this work is to evaluate the surface properties of the alloy, detailed consideration about the substrate will be omitted.

### 3.3. Electrochemical characterisation

The electrochemical characterisation was performed in order to evaluate the protective effectiveness of the surface layers formed on the alloy during etching and heat treatment. Three techniques were used: surface resistance measurements, cyclic polarisation and open-circuit potential measurements.

The surface of mirror polished samples presents, after chemical treatment in NaOH (MA), a high electrical resistance with a minimum value measured of  $20\text{ G}\Omega$ . The layer resistance decreases dramatically for MA600, MA700 and MA800 samples (respectively  $5\text{ M}\Omega$ ,  $6\text{ M}\Omega$ ,  $1\text{ M}\Omega$ ), but they are still insulating; on the contrary all the sandblasted samples exhibit a high electrical

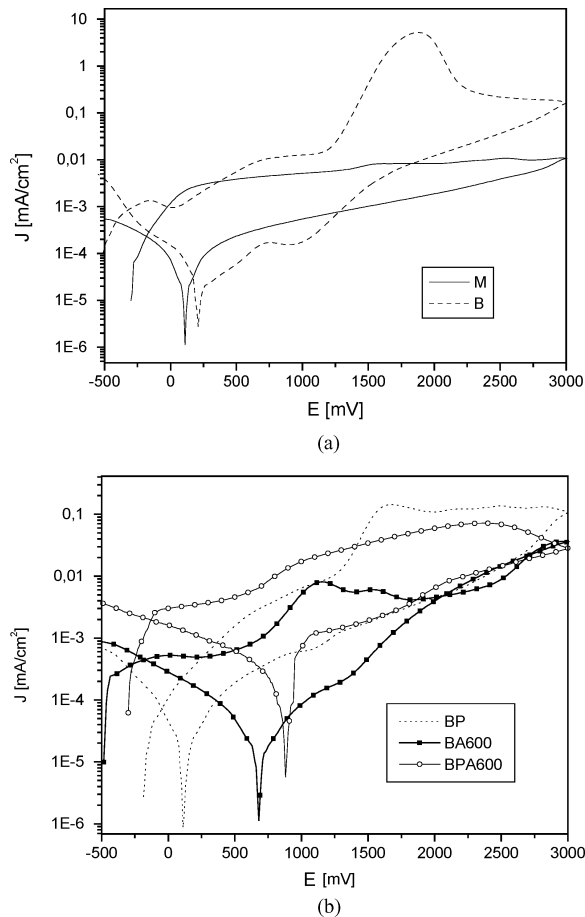


Figure 6 Layer a: Cyclic polarisation curves related to mechanically treated samples (*M* and *B* series). Layer b: Polarization curves obtained on the *BA600*, *BP* and *BPA600* samples.

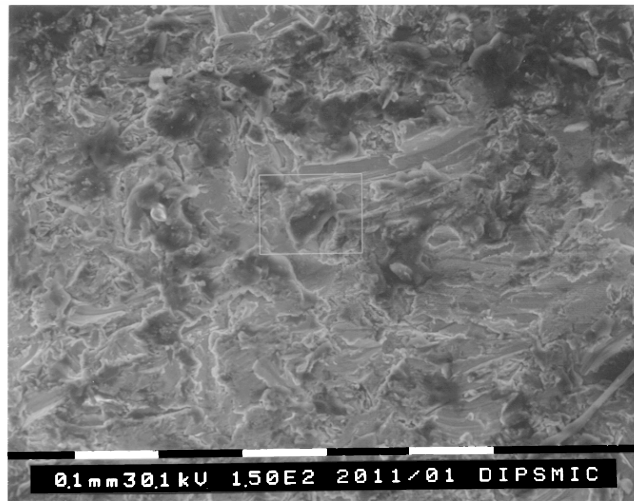
conductivity. It must be evidenced that these measurements present a relevant dispersion of the results due to the mechanical instability of the surface layers that are damaged by the metallic tip used for the measure. The data reported are the results of a mathematical average between minimum values obtained.

The cyclic polarisation curves related to mechanically treated samples, that means the as-polished (*M*) and sandblasted (*B*) series, are reported in Fig. 6—layer a. The current density values were obtained by considering the geometrical area of the electrodes, even if the real surface area of sandblasted samples is slightly greater than that of mirror polished ones. The polished sample presents low current density, due to the presence of a native passive film. On the contrary the *B* sample presents higher current density and does not remain passive during the polarisation experiment, showing a current peak centred at +1750 mV (SCE). The polarization curves obtained on the alkali and heat treated samples (*BA600*), passivated samples (*BP*) and samples treated by two step chemical etching and heat treatment (*BPA600*) are reported in Fig. 6—layer b. The samples heat-treated at 600 °C were selected by considering morphology and crystallographic structure data previously shown. As previously shown the polished and alkali treated samples present on the surface an insulating layer that remains non-conductive also after heat treatment at 600 °C. As consequence it was impossible to perform polarisation experiments on these samples

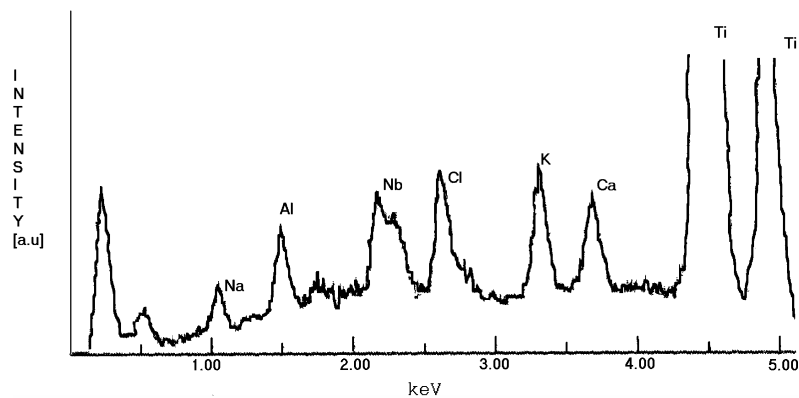
(*MA*, *MA600*). It can be noted, by observation of polarisation curves, that the samples treated by alkali or two step etching and heat treatment (*BA600*, *BPA600*) present low current density on the whole potential range explored and behaviour similar to that of the *M* sample. The *BA600* sample presents an hysteresis loop at high positive potential, confirming that the surface layer is not damaged by the potential excursion and the sample is further passivated. The *BP* sample shows an intermediate behaviour between the *BA600* and *B* sample, with a value of about 0.1 mA/cm<sup>2</sup> as maximum density current level.  $E_{\text{prot}}$ , the potential value below which the material is not subjected to corrosion attack, is an interesting parameter in order to compare the damage resistance capability of the surface layer. From the cyclic polarisation curves one observes that  $E_{\text{prot}}$  is much positive as higher the layer resistance is and it presents the highest values in the case of the *BPA600* (880 mV) and *BA600* (700 mV) samples, while it is comprised among 100 and 200 mV in the other cases.

All the samples were observed by SEM after anodic polarisation. A lot of dark regions, about 50 μm in dimension, can be observed on the surface of the *BP* sample (Fig. 7(a)). The EDS analysis shows that they contain Na, Cl, K, Ca, further the element of the alloy (Fig. 7(b)), so they can be considered as zones prone to pitting corrosion. Some pits are also observable randomly on the *B* surface, while no corrosion products can be observed on the *M*, *BA600* and *BPA600* samples subjected to anodic polarisation. On the *BA600* and *BPA600* samples the surface layer due to the thermochemical treatment is still observable at high magnification, confirming that it was not damaged during the anodic polarisation.

The E-t curves obtained by means of open-circuit potential measurements are reported in Fig. 8. This test is interesting in order to assess the protective ability and stability of the surface passivation layers when exposed to physiologic solution. A first comparison can be performed by observing the free corrosion potential ( $E_{\text{corr}}$ ) at the beginning of the measure: the surface is much more protective as higher is the  $E_{\text{corr}}$  value. The lowest value of  $E_{\text{corr}}$ , at the immersion of the electrode in the Ringer solution, is shown by the *B* sample (−407 mV), which exposes on the surface a damaged oxide layer. On the contrary the highest value at  $t = 0$  is shown by the *BP* electrode (−131 mV), due to the presence of a thick oxide layer produced by the passivation treatment performed in HNO<sub>3</sub>. The samples treated by alkali or two-step etching and heat treatment (*BA600*, *BPA600*) present higher values than the polished (*M*) electrode (−281 mV in the case of *BA600* and −218 mV in the case of *BPA600*), according to the presence of the surface layers formed during the thermochemical treatments. On the other side the sequence of  $E_{\text{corr}}$  values recorded after 72 h, starting from the lowest up to the highest, is: *BA600*, *M*, *BP*, *BPA600* and *B*. This sequence can be interpreted as a progressive increase in the protective ability of the surface layer. During the test the *M* and *BP* samples show a quite stable behaviour, while on the contrary the *B* sample appears as quite reactive. The electrodes treated by alkali or two-step



(a)



(b)

Figure 7 Surface morphology (a) and EDS analysis (b) of a BP sample after anodic polarisation.

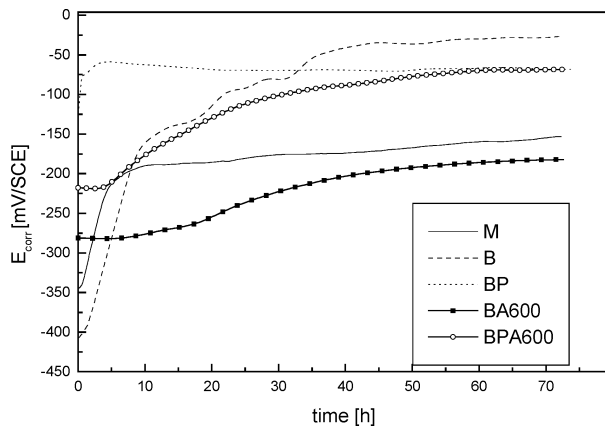


Figure 8 E-t curves obtained by means of open-circuit potential measurements (M, B, BP, BA600, BPA600 samples).

etching and heat treatment (BA600, BPA600) show a moderate reactivity with the Ringer solution.

All the electrodes were observed by means of SEM-EDX after the open-circuit potential measurements. No evident morphological or compositional changes, due to the exposition to the Ringer solution, were detected.

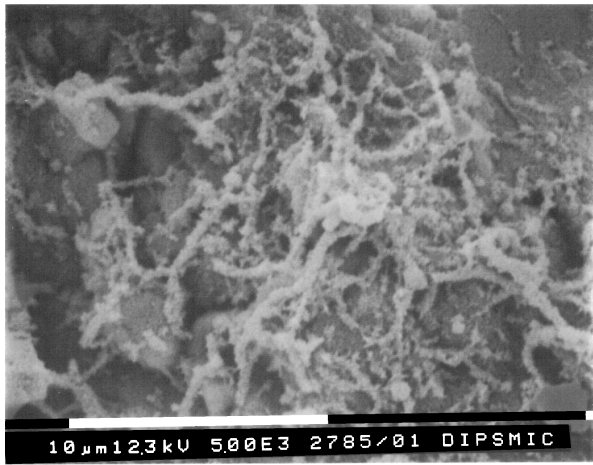
### 3.4. Bioactivity

The bioactive ability of the treated samples has been tested by *in vitro* experiments. The presence of a reaction

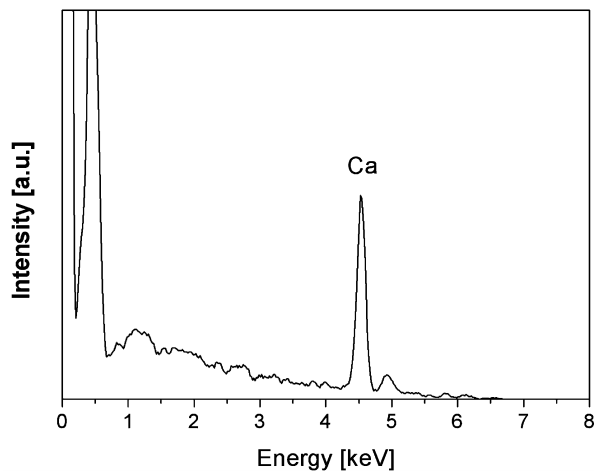
layer containing Ca, as aggregation of small crystals, was detected, by means of EDX analysis, on the surface of samples treated by alkali or two step etching and heat treatment (MA600, BA600, BPA600) after 5 days soaking in SBF (Fig. 9). Well developed precipitated crystals, containing Ca and P, were detected on the same samples after 14 days of soaking in SBF. No evidence of surface modification due to soaking was registered on the sandblasted and passivated (BP) series, used as reference. The crystals are present, on the bioactive samples observed, as randomly dispersed island. They are about 2–4  $\mu\text{m}$  in diameter (Fig. 10) and present a P content slightly lower respect to the nominal HAp composition. The morphology resembles that of apatite. The presence of a polished or of a blasted substrate does not seem to influence the bioactivity of the surface layer. On the other hand it must be underlined that these data are not entirely reproducible and treated samples presenting no bioactive ability were randomly observed.

## 4. Discussion

The first aim of this work was to investigate the bioactive ability of the Ti-6Al-7Nb alloy after alkali and heat treatments, analogously to the investigation reported in literature on pure titanium and some others alloys. The substrate roughness was considered as a variable. Mirror polished and sandblasted surfaces



(a)



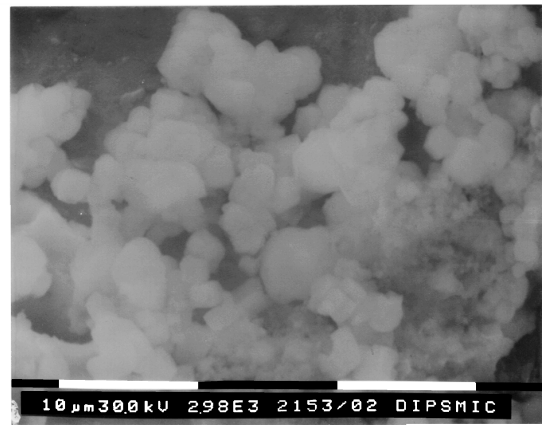
(b)

Figure 9 Aggregates of precipitated crystals on BPAV sample after 5 days of soaking. a) SEM microphotograph b) EDS analysis

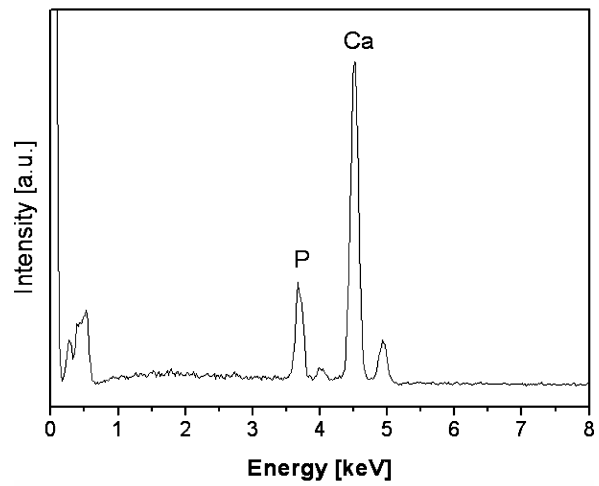
were investigated, because both these surface states are actually used on implants and they are representative of two opposite mechanical surface states. Thermochemical treatments on sandblasted surfaces are of particular interest also because they can be applied uniformly on complicated surface topography of substrate, where plasma-spraying coating is difficult. So they are promising treatments in order to obtain surface with good bone-bond ability and appropriate topography for cementless prosthesis. Nevertheless it must be considered that the surface properties of sandblasted titanium alloys are not completely analogous to those of mechanical or electropolished surfaces, because of chemical modifications due to mechanical damage [18], so their properties and behaviour must be investigated in a specified way.

On the other hand the corrosion resistance of the microporous surface layer produced by the thermochemical treatments was investigated in detail during this work, in order to clarify if it is an efficient protective barrier as the native titanium oxide is. A new two-step treatment was tested in order to improve the anticorrosion performances of the bioactive titanium alloy.

Considering the single step treatment, the morphological and structural analysis, performed during this work, evidenced that both on the mirror polished and the



(a)



(b)

Figure 10 Crystals nucleated and growth on a blasted, passivated, alkali and heat treated sample (BPA600) after 14 days soaking in SBF. a) SEM microphotograph b) EDS analysis

sandblasted surfaces of the Ti-6Al-7Nb alloy it is possible to obtain the formation of a microporous layer by alkali and heat treatment. The substrate roughness influences slightly the characteristics of the surface layer formed on treated samples with different mechanical state (MA600, BA600). In the case of mirror polished samples the morphology is different by using a passivation pre-treatment or not (MPA600, MA600), while in the case of blasted samples it is alike in both cases (BPA600, BA600). From the structural point of view our data revealed that an increase in substrate roughness causes a higher degree of crystalline fraction on the treated surfaces. This effect can be explained considering that the fraction of crystals, formed by crystallization of the amorphous hydrogel, depends on the number of nucleation sites. It is well known [22, 23] that the number of crystalline nuclei is efficiently increased on the surface of glasses by the presence of sharp tips or edges due to mechanical damaging. On the other hand it was evidenced by others authors that the degree of oxidation of metals during heat treatment is related to their surface roughness and mechanical treatment [24]. Cold work and blasting increase the degree of oxidation at a fixed temperature. The data reported in literature up today on bioactive titanium were obtained on mechanically grinded surfaces (400 grid size), with

a surface roughness intermediate among the two states considered in this work. It can be concluded that the best conditions of thermochemical treatment (concentration of the NaOH solution, etching time, temperature of subsequent heat treatment) must be opportunely determined case by case.

The cyclic polarisation test provides important information about the stability of the surface layers when exposed to aggressive environments. Using as reference the quite firm native oxide formed on polished surface, a comparison can be performed by the observation of the values of the passive current density. Surface damage due to blasting is relevant and not cancelled by air exposure. A protective surface layer is partially recovered by passivation treatment in HNO<sub>3</sub> and more efficiently by alkali or two step etching and heat treatment. The surface layer formed by these treatments appears to be, on blasted samples, as resistant as the native one on smooth samples is. Furthermore a higher value of  $E_{\text{prot}}$  has been found in the case of *BA600* and *BPA600*, indicating a better damage resistance than the *M* one. Cases of pitting were found on *BP* samples, revealing that the passivation treatment performed in HNO<sub>3</sub> is not completely adequate and involves the release of corrosion products.

Complementary information may be obtained by open-circuit potential measurements ( $E_{\text{corr}}$ ), which provide information about the stability and durability of the surface layer when exposed to physiologic solution. The *BA600* surface presents a low free corrosion potential, so it must be evidenced that it shows a reduced protective effectiveness against substrate corrosion and ion release. This could be related to its porous nature and thin thickness. The increment of ion release from rough surfaces represents a well-known problem to the scientific literature [25] and the alkali and heat treatment does not appear to be an adequate solution at this concern. The presence of insulating layers on the *MA600* samples could be an indication that this behaviour is avoided when smooth substrates are alkali and heat-treated. Detailed ion release investigations are necessary in order to clarify this aspect. On the contrary the passivation treatment performed in HNO<sub>3</sub>, nowadays employed on titanium implants, seems to produce a thick, stable and protective oxide layers, but, as previously underlined, the surface is more prone to pitting when exposed to aggressive environments. The best protective effectiveness is shown by the sample treated by two step chemical etching and heat treatment (*BPA600*) that exhibits, at the same time, a wide passive region and an high protection potential value during cyclic polarisation, together with high free corrosion potential values during immersion in Ringer solution. Its behaviour can be considered better both respect to the passivated sample (*BP*), that presents evidences of pitting corrosion after cyclic polarisation and respect to the alkali and heat treated one (*BA600*), that has quite low free corrosion potential values. The two-step chemical etching seems to be an efficient method in order to produce a microporous layer, by alkali treatment, on a protective passive surface formed by passivation in nitric acid.

Considering the bioactive ability, it was verified that alkali and heat treatment are effective also on the Ti-6Al-7Nb alloy and on previously passivated samples. The aim is to obtain metal implants forming an apatite layer on their surface, by taking calcium and phosphate ions from the surrounding body fluid, and so easily bonded to the living bone. The formation mechanism of the hydroxylapatite crystals seems to be quite similar to what already reported by other authors [26], with the deposition of Ca<sup>++</sup> ions at first time, due to the presence of a negative surface charge, and of phosphate ions in a second step. As it was recently proposed the metal induces apatite formation via amorphous calcium titanate and calcium phosphate as precursors [27]. The effect of the presence of Na on the treated surfaces, respect to the bioactive mechanism, is still on discussion. In fact it was reported that also titania gel, without sodium ions, shows bioactive ability via phosphate and calcium ion bonding [28]. According to these data we observed bioactive ability on samples showing reduced Na presence only on a quite thin surface layer [29]. Otherwise it must be underlined that these data are affected by not complete reproducibility when performed in different labs. The presence of alumina particles on blasted surfaces seems not to be a critical factor respect to bioactive ability, because of the analogous behaviour of mirror polished and blasted materials.

Considering that the bioactive ability of the sample treated by two-step chemical etching and heat treatment is comparable with that of alkali and heat treated ones, it can be considered a promising material presenting at the same time good anticorrosion performance and bioactive behaviour. This new preparative method is quite different from the two-step method proposed by H.B.Wen *et al.* [8] first of all because it is simpler, and does not involve pressure process, and because of the use of nitric acid instead of HCl and H<sub>2</sub>SO<sub>4</sub>.

Further studies will be performed in order to establish the entity of ion release from surfaces treated by single or two step etching and with different mechanical state. Cytotoxicity tests on these samples are also in progress.

## 5. Conclusions

It can be concluded that the Ti-6Al-7Nb alloy presents bioactive ability and good corrosion resistance after an appropriate surface treatment, consisting on a two-step chemical etching and heat treatment. The treatment described is effective both on polished and on blasted surfaces, but the conditions employed must be set considering the roughness of the substrate. The two-step chemical and heat treatment allows to obtain a surface presenting better performance than the passivated one, because of its bone-bonding ability, and than the single step chemical and heat treated one, because of its good corrosion resistance.

## Acknowledgments

The Centerpulse Orthopedics and the Synos Foundation are acknowledged for the research grant and the material kindly supplied.



## References

1. H. B. WEN, J. G. C. WOLKE, J. R. DE WIJN, Q. LIU, F. Z. CUI and K. DE GROOT, *Biomater.* **18** (1997) 1471.
2. H. M. KIM, F. MIYAJI, T. KOKUBO and T. NAKAMURA, *J. Mat. Sci. Mat. Med.* **8** (1997) 341.
3. B. C. YANG, J. WENG, X. D. LI and X. D. ZHANG, *J. Biomed. Mat. Res.* **47** (1999) 213.
4. M. FINI, A. CIGADA, G. RONDELLI, R. CHIESA and R. GIARDINO, *Biomaterials* **20** (1999) 1587.
5. T. KOKUBO, H.-M. KIM, S. NISHIGUCHI and T. NAKAMURA, *Key Eng. Mat.* **192–195** (2001) 3.
6. H. K. KIM, Y. SASAKI, J. SUZUKI, S. FUJIBAYASHI, T. KOKUBO, T. MATSUSHITA and T. NAKAMURA, *ibid.* **192–195** (2001) 227.
7. C. OHTSUKI, H. IIDA, S. HAYAKAWA and A. OSAKA, *J. Biomed. Mater. Res.* **35** (1997) 39.
8. H. B. WEN, Q. LIU, J. R. DE WIJN, K. DE GROOT and F. Z. CUI, *J. Mat. Sci. Mat. Med.* **9** (1998) 121.
9. T. KOKUBO, F. MIYAJI and H. M. KIM, *J. Am. Ceram. Soc.* **79** (1996) 1127.
10. H. M. KIM, F. MIYAJI, T. KOKUBO and T. NAKAMURA, *J. Biomed. Mater. Res.* **38** (1997) 121.
11. H. M. KIM, F. MIYAJI, T. KOKUBO, S. NISHIGUCHI and T. NAKAMURA, *ibid.* **45** (1999) 100.
12. H. M. KIM, H. TAKADAMA, T. KOKUBO, S. NISHIGUCHI and T. NAKAMURA, *Biomater.* **21** (2000) 353.
13. W. Q. YAN, T. NAKAMURA, M. KOBAYASHI, H. M. KIM, F. MIYAJI and T. KOKUBO, *J. Biomed. Mater. Res.* **37** (1997) 267.
14. S. NISHIGUCHI, T. NAKAMURA, M. KOBAYASHI, H. M. KIM, F. MIYAJI and T. KOKUBO, *Biomater.* **20** (1999) 491.
15. T. MIYAZAKI, H. M. KIM, F. MIYAJI, T. KOKUBO, H. KATO and T. NAKAMURA, *J. Biomed. Mater. Res.* **50** (2000) 35.
16. H. KATO, T. NAKAMURA, S. NISHIGUCHI, Y. MATSUSUE, M. KOBAYASHI, T. MIYAZAKI, H. M. KIM and T. KOKUBO, *ibid.* **53** (2000) 28.
17. H. M. KIM, F. MIYAJI, T. KOKUBO and T. NAKAMURA, *ibid.* **32** (1996) 409.
18. K. ANSELME, P. LINEZ, M. BIGERELLE, D. LEMAGUER, A. LEMAGUER, P. HARDOUIN, H. F. HILDEBRAND and A. IOST, *J. M. Leroy Biomater.* **21** (2000) 1567.
19. M. SVEHLA, P. MORBERG, B. ZICAT, W. BRUCE, D. SONNABEND and W. R. WALSH, *J. Biomed. Mater. Res.* **51** (2000) 15.
20. N. VERDONSCHOT, E. TANCK and R. HUISKES, *ibid.* **42**, (1998) 554.
21. P. SCARDI, M. LEONI, B. TESI, C. GIANOGLIO and T. BACCI, *Surf. Eng.* **14** (1998) 513.
22. N. DIAZ-MORA, E. D. ZANOTTO, R. HERGT and R. MULLER, *J. Non-Cryst. Sol.* **273** (2000) 81.
23. R. MULLER, *ibid.* **219** (1997) 110.
24. W. J. TOMLINSON and K. BLICK, *J. Mat. Sci. Lett.* **9** (1990) 1005.
25. J. Y. MARTIN, Z. SCHWARTZ, T. W. HUMMERT, D. M. SCHRAUB, J. SIMPSON, J. LANKFORD JR, D. D. DEAN, D. L. COCHRAN and B. D. BOYAN, *J. Biomed. Mater. Res.* **29** (1995) 389.
26. B. C. YANG, J. WENG, X. D. LI and X. D. ZHANG, *ibid.* **47** (1999) 213.
27. H. TAKADAMA, H.-M. KIM, T. KOKUBO and T. NAKAMURA, *Key Eng. Mat.* **192–195** (2001) 51.
28. P. LI, I. KANGASNIEMI, K. DE GROOT and T. KOKUBO, *J. Am. Ceram. Soc.* **77** (1994) 1307.
29. S. SPRIANO, M. BRONZONI, E. VERNÈ, G. MAINA, V. BERGO and M. WINDLER, "Characterization of Surface Modified Ti-6Al-7Nb Alloy" submitted to *J. Mat. Sci. Mat. Med.*

Received 31 December 2003

and accepted 12 August 2004